

# Quantum chaos meets quantum channels

September 10, 2024

## 1 Model

The spin chain we are interested in studying first is that studied by Mirkin and Wisniacki in Ref. [1]:

$$H = \sum_{i=1}^L (h_x \sigma_i^x + h_z \sigma_i^z) - \sum_{i=1}^{L-1} J_z \sigma_i^z \sigma_{i+1}^z. \quad \text{eq:H:wisniacki:ising:chain} \quad (1)$$

## 2 Mean level spacing ratio

The level spacing ratio  $\tilde{r}_n$  is defined as:

$$\tilde{r}_n = \frac{\min(s_n, s_{n-1})}{\max(s_n, s_{n-1})}, \quad \text{eq:level:spacing:ratio} \quad (2)$$

where  $s_n = E_{n+1} - E_n$ . The mean level spacing ratio  $\langle \tilde{r}_n \rangle$  is known to attain the value  $\langle \tilde{r}_n \rangle \approx 0.5207$  when the level spacing distribution  $P(s)$  is Wigner-Dyson and  $\langle \tilde{r}_n \rangle \approx 0.386$  when it is Poisson.

## 3 Spectral form factor

The spectral form factor  $K(t)$  is defined as:

$$K(t) = \frac{1}{2^L} \left\langle |\text{Tr } U(t)|^2 \right\rangle = \frac{1}{2^L} \left\langle \sum_{i,j} e^{i(E_i - E_j)t} \right\rangle, \quad \text{eq:sff} \quad (3)$$

where  $\langle \cdot \rangle$  denotes the ensemble-average over statistically-similar systems.

## 4 Chaometer's quantum channel

The reduced dynamics of the chaometer is described by the quantum channel:

$$\mathcal{E}(\rho) = \text{Tr}_E \left( e^{-iHt} \rho \otimes \left| \psi_0^{(E)} \right\rangle \left\langle \psi_0^{(E)} \right| e^{iHt} \right), \quad (4)$$

where  $H$  is that of eq. (1),  $\left| \psi_0^{(E)} \right\rangle$  the initial state of all spins except the chaometer, and  $\rho$  the initial state of the chaometer.

The chaometer's quantum channel  $\mathcal{E}$ , in general, is divisible into:

1. A unitary operation rotating the Bloch's sphere.
2. A quantum channel that deforms the Bloch's sphere and translates its origin.

Both operations do not commute.

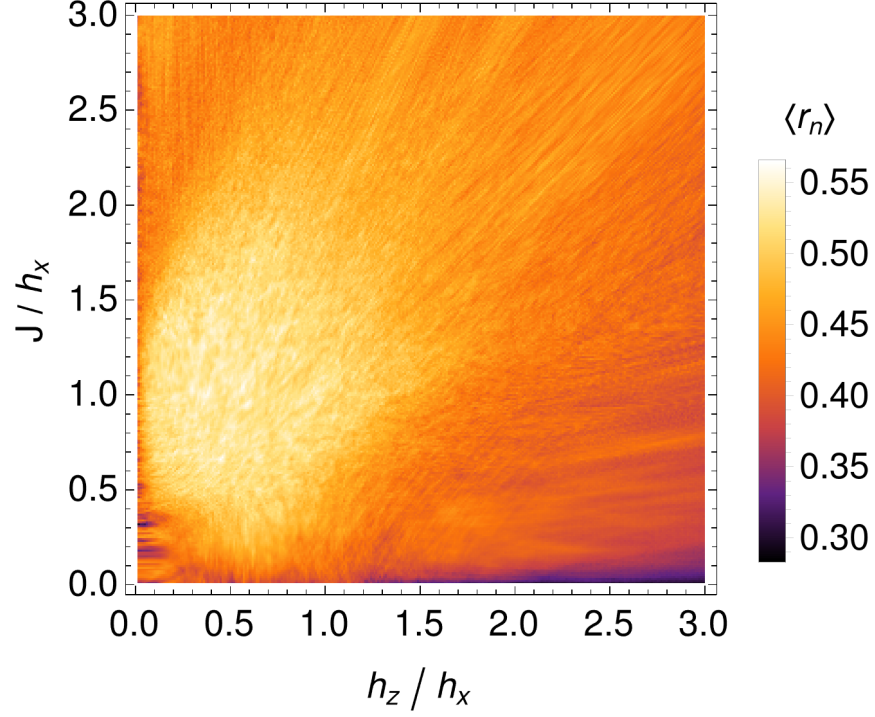


Figure 1: Mean level spacing ratio  $\langle \tilde{r}_n \rangle$  [c.f. eq. (2)] of the Ising chain with Hamiltonian (1) as a function of ratios  $h_z/h_x$  and  $J/h_x$ . We assume  $J_z = J \forall k$ . fig:mean:level:spacing:ratio

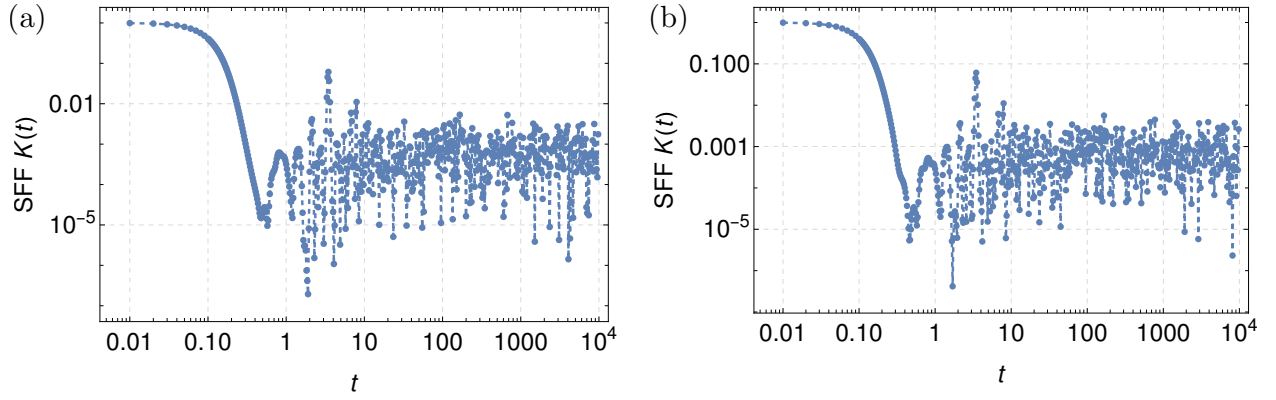


Figure 2: Spectral form factor (SFF) [c.f. (3)] in regular region:  $h_z/h_x = 2.5$  and  $J/h_x = 1$ . (a) Whole spectrum. (b) Even-parity subspace spectrum. fig:sff:regular

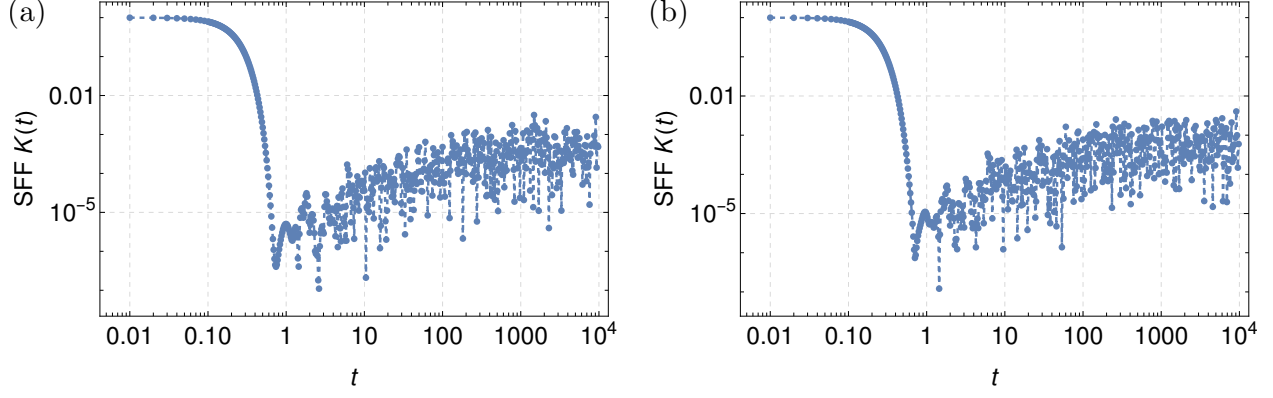


Figure 3: Spectral form factor (SFF) [c.f. (3)] in chaotic region:  $h_z/h_x = 0.5$  and  $J/h_x = 1$ . (a) Whole spectrum. (b) Even-parity subspace spectrum. fig:sff:chaotic

## 5 Purity of the chaometer

Averaged purity  $\mathcal{P}$  is defined in Ref. [1] as:

$$\bar{\mathcal{P}} = \frac{1}{N} \sum_{i=1}^N \left( \frac{1}{T} \int_0^T \text{Tr} [\rho_i^2(t)] \right) \quad \text{eq:avg:purity} \quad (5)$$

where:

- $\rho_i(t)$ : chaometer's density matrix.
- $N$ : number of different random initial states of the whole chain.  $N = 50$  in Mirkin and Wisniacki [1].
- $T$ : maximum time.  $T = 50$  in Mirkin and Wisniacki [1].

Also, the normalized averaged purity is defined as

$$\bar{\mathcal{P}}_{Norm} = \frac{\bar{\mathcal{P}} - \min(\bar{\mathcal{P}})}{\max(\bar{\mathcal{P}}) - \min(\bar{\mathcal{P}})}, \quad \text{eq:avg:norm:purity} \quad (6)$$

where  $\max(\bar{\mathcal{P}})$  and  $\min(\bar{\mathcal{P}})$  are the minimum and maximum value obtained when sweeping the parameter range ( $h_z$  in their case).

In Fig. 4 we plot one realization of the dynamics of purity of the chaometer. We compare in Fig. 5 our results and those of Mirkin and Wisniacki [1].

## 6 Purity of Choi matrix

We investigate the purity of Choi matrix of the quantum channel  $\mathcal{E}(t)$  of the chaometer in Fig. 6.

$$\text{Tr} \{ [\mathcal{E}^R(t)/2]^2 \} \quad (7)$$

JA: Comentar el problema de la normalización de Mirkin y Wisniacki y que parece que se resuelve aquí

## 7 Non complete positiveness of $\Lambda(t, s)$

Any quantum channel  $\mathcal{E}(t)$  can composed as

$$\mathcal{E}(t) = \Lambda(t, s) \circ \mathcal{E}(s, 0), \quad \text{eq:Lambda} \quad (8)$$

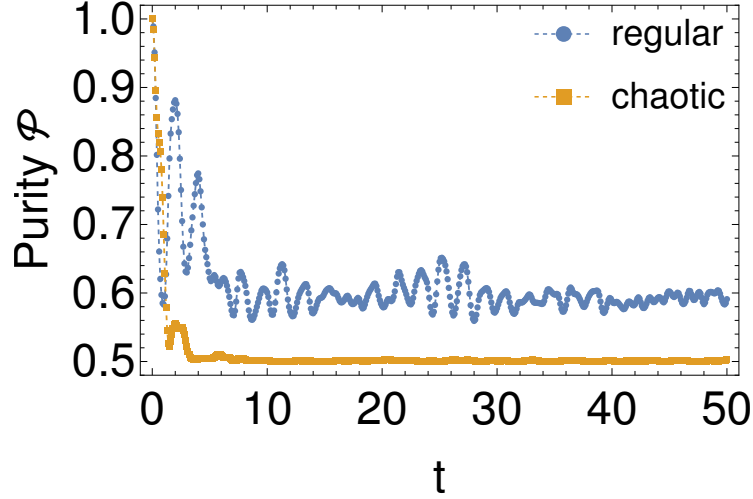


Figure 4: Dynamics of chaometer's purity of a single realization with the same initial state of the environment of the first chaometer's quantum channel of the videos. fig:purity:one:realization

46 nonetheless,  $\Lambda(t, s)$  is not in general completely positive. A way to quantify how far is  $\Lambda(t, s)$  from being  
 47 completely positive is through  $\tilde{\lambda}$ : eq:lambda:tilde

$$48 \quad \tilde{\lambda} = |\min(0, \lambda_{\text{smallest}})|, \quad (9)$$

49 where  $\lambda_{\text{smallest}}$  is the smallest eigenvalue of  $\Lambda^R(t, s)/2$ . We have added the factor  $1/2$  just so  $\text{Tr}[\Lambda^R(t, s)/2] = 1$ .

50 Let us fix  $s = 0.1$  and investigate the complete positiveness of  $\Lambda(t, s)$ , see Fig. 7.

## 51 References

- 52 [1] Nicolás Mirkin and Diego Wisniacki. Quantum chaos, equilibration, and control in extremely short spin  
 53 chains. *Phys. Rev. E*, 103:L020201, Feb 2021.

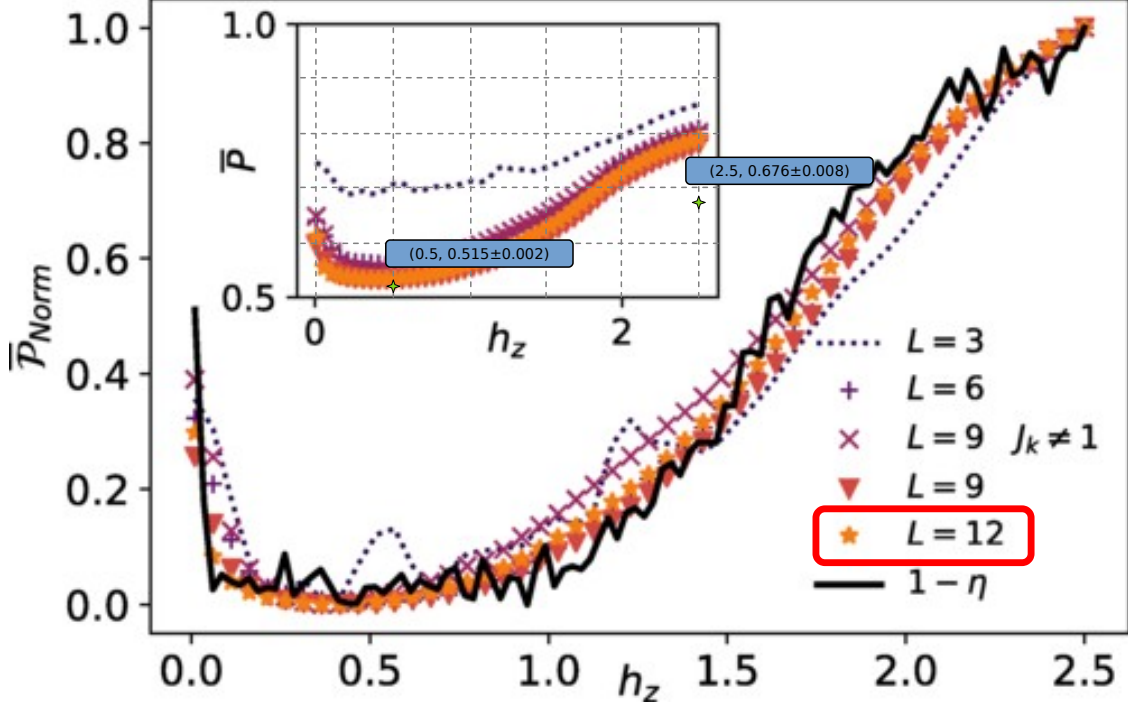


Figure 5: Averaged  $\bar{P}$  and averaged normalized purities  $\bar{P}_{Norm}$  [c.f. eqs. (5) and (6).] for  $N = 50$  random initial states of the chaometer for each quantum channel showed in the videos. JA: Tendría más sentido sacar la pureza del canal. Lo pienso Taken and modified from Ref. [1]. fig:mirkin2021:fig2:modified

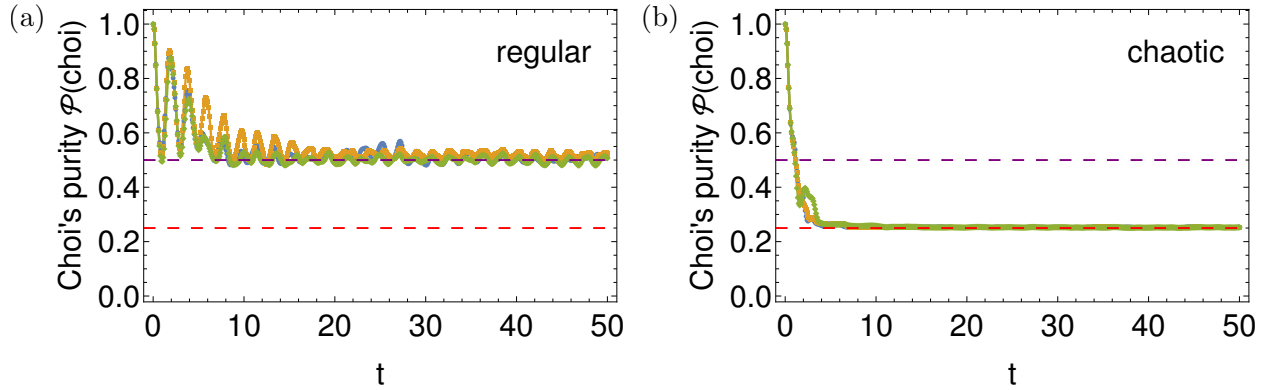


Figure 6: Purity of Choi matrix in (a) regular ( $h_z = 2.5$ ) and (b) chaotic ( $h_z = 0.5$ ) for the three random initial states showed in the video. fig:choi:purity

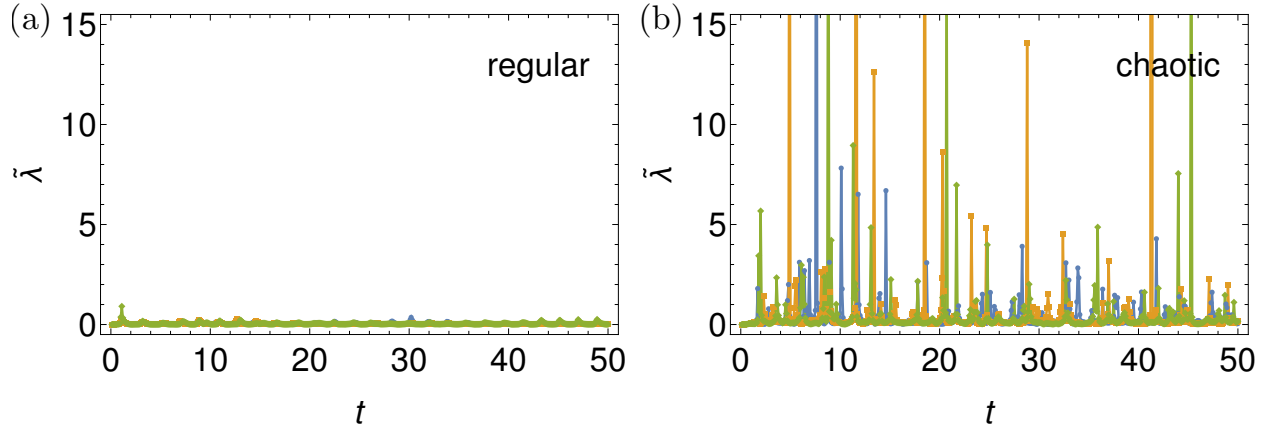


Figure 7: Most negative eigenvalue  $\tilde{\lambda}$  of map  $\Lambda(t, s)/2$ , with  $s = 0.1$  [c.f. eqs. (8) and (9)]. *fig:lambs-tilde:choi*

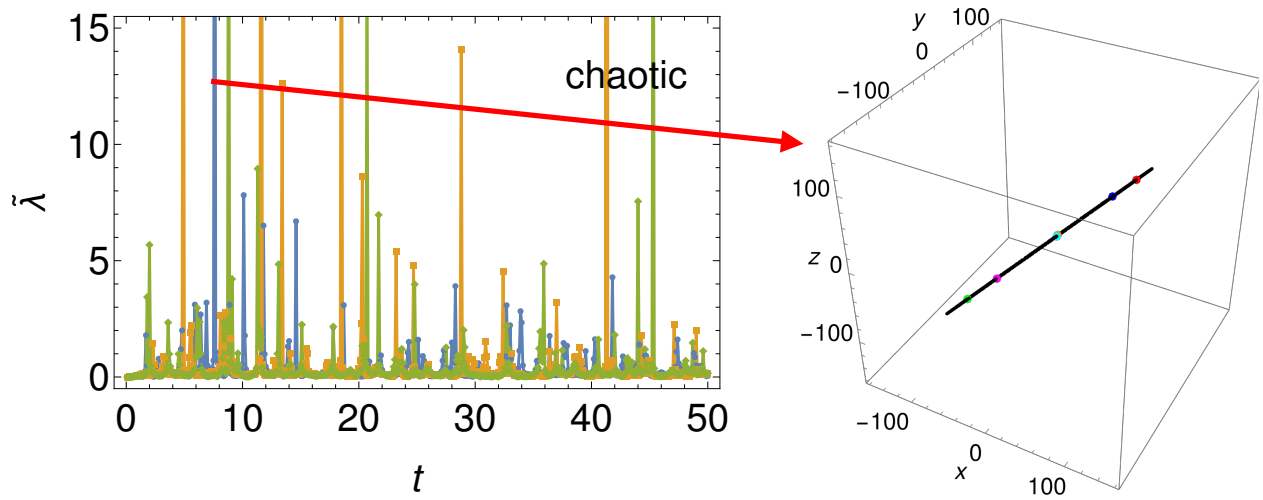


Figure 8: Burst of the Bloch sphere at  $t = 0.5$  s. *fig:burst*